Supplementary Information

"Reconciliation of observation- and inventory- based CH_4 emissions for eight large global emitters"

1. Data products

$CoCO_2$ (https://coco2-project.eu/) is a scientific collaborative effort funded by the H2020 European Commissions, grant number 958927. This synthesis has been originally based on data and country specific plots from previous VERIFY project, for the EU27: https://webportals.ipsl.fr/VERIFY/FactSheets, v1.28 and on the WP8 deliverable Reports D8.1 (https://coco2-project.eu/node/333) and D8.2 (https://coco2-project.eu/node/360) from the $CoCO_2$ project website. The data behind all figures is found at: https://doi.org/10.5281/zenodo.10276087, (Petrescu et al., 2023b)

We used BU anthropogenic emissions from national inventory reports (NIRs and CRFs) (UNFCCC NGHGI, 2023) and global datasets covering all sectors (EDGAR v7.0, GAINS (no IPPU), FAOSTAT-PRIMAP).

Natural CH_4 emissions from the VERIFY synthesis (Petrescu et al., 2023a) were used for the EU27 analysis and belong to biogeochemical models of wetlands/peatlands and mineral soil emissions (JSBACH-HIMMELI), inland waters (lakes, rivers and reservoirs) plus updated data for the RECCAP2 project (Lauerwald et al., 2023), updated activity data for total geological emissions here in SI (based on Etiope et al., 2019) and biomass burning from GFEDv4.1s (van der Werf et al., 2017). Global natural wetlands emissions belong to LPJ-GUESS and inland waters (global lakes & reservoirs) to ORNL DAAC (Johnson et al., 2021, 2022) (see Table S1).

TD approaches include both regional and global inversions, the latter having a coarser spatial resolution. These estimates are described in the following Table S1.

Table S1: Data sources for CH_4 emissions used in this study:

Name	Domain	Description	Contact / lab	References	Status compared to Petrescu et al., 2023a and D8.2
CH_4 Bottom-up anthropogenic					
UNFCCC NGHGI (2023) CRFs and BURs	EU27	CH_4 emissions 1990-2021	MS inventory agencies Yearly uncertainties provided by the EU GHG inventory team	UNFCCC CRFs https://unfccc.int/ghg-inventories-annex-i-parties/2023 UNFCCC BURs https://unfccc.int/BURs	Updated
EDGAR v7.0	EU27 and global	Total and sectoral global CH4 emissions 1990-2021	EC-JRC	Crippa et al., 2020 Crippa et al., 2019 JRC report Janssens-Maenhout et al., 2019 Solazzo et al., 2021	Updated
GAINS	EU27 and global	Total and sectoral global CH4 emissions 1990-2020	IIASA	Höglund-Isaksson, L. 2017 Höglund-Isaksson, L. et al., 2020	Updated
FAOSTAT	EU27 and global	Global CH_4 agriculture and land use emissions, as well as for other sectors (based on PRIMAP) 1990-2020	FAO	Tubiello et al. 2013 Tubiello, 2019, 2022 FAO, 2015, 2023	Updated

CH_4 bottom-up natural					
LPJ-GUESS	Global	Global CH4 emissions from wetlands 1990-2021	U Lund	Wania et al., 2009 Wania et al., 2010 Spahni et al., 2011 Zhang et al., 2021	New
JSBACH-HIMMELI	EU27	European CH4 emissions from peatlands and mineral soils 2005-2020	FMI	Raivonen et al., 2017 Susiluoto et al., 2018	Not updated
DAAC ORNL	Global	Global CH4 emissions from lakes (2003-2015) and dam-reservoirs (2002-2015)	NASA	Johnson et al. 2021 and 2022	New
Geological emissions	Global	Global grid geological CH_4 emission model (2019)	Istituto Nazionale di Geofisica e Vulcanologia (INGV)	Etiope et al., 2019 and current work (updated activity data)	Updated
GFED4.1s	Global	Biomass burning global CH4 emissions 2000-2020	VU Amsterdam	van der Werf et al., 2017	not updated
CH_4 top-down natural and anthropogenic					
FLExKF-v2023	EU27	Regional total CH_4 emissions from inversions with uncertainty 2005-2021	EMPA	Brunner et al., 2012 Brunner et al., 2017 Segers et al., 2020	Updated
CAMS v21r1	Global	Total and source split partitions for global CH_4 emissions NOAA (1979-2021) NOAA_GOSAT (2009-2021)	TNO	Huijnen et al., 2010 Pandey et al., 2022 Segers et al., 2022	New
CTE-GCP2021	Global	Total global CH_4 emissions with source split partitions and posterior flux uncertainty 2000-2020	FMI	Bruhwiler et al., 2014 Houweling et al., 2014 Giglio et al., 2013 Ito et al., 2012 Janssens-Maenhout et al., 2013 Krol et al., 2005 Peters et al., 2005 Saunois et al., 2020 Stocker et al., 2014 Tsuruta et al., 2017	New
CIF-CHIMERE and CIF-FLEXPARTv10.4	EU27	Total regional CH_4 emissions from inversions CHIMERE: 2005-2022 FLEXPART: 2005-2020	LSCE, NILU	Berchet et al., 2021 Fortems-Cheiney et al., 2021	New and updated
MIROC4-ACTM (control and OH varying runs)	Global	Total and source split partitions for global CH_4 emissions (2 runs: control and variable OH) 2001-2021	JAMSTEC	Patra et al., 2021 Chandra et al., 2021	New
TM5-4DVAR (TROPOMI)	Global	Total and source split partitions for global CH_4 emissions May2018-2020	VUA	Huijnen et al., 2010 Lorente et al., 2023	New
GEOS-Chem CTM (TROPOMI for USA)	USA	Total CH_4 emissions for USA 2019	Harvard University	Nesser et al., 2023	New
CEOS (GOSAT)	Global	Total and source split partitions for global CH4 emissions 2019	NASA/JPL	Worden et al., 2019	New

The following BU anthropogenic data products used in this paper are described in detail in Petrescu et al., 2023a, Appendix A1.1: UNFCCC NGHGIs, EDGAR, GAINS and FAOSTAT

The natural CH_4 products are described in Petrescu et al., 2023a, Appendix A2.1: inland waters and JSBACH-HIMMELI.

The following TD data products are described in Petrescu et al., 2023a, Appendix A1.2: VERIFY CIF framework (Berchet et al., 2021), CTE-GCP, MIROC4-ACTM.

Priors used by different products are found in the zenodo link:

Table S2: Source-specific activity data (AD), emission factors (EF), uncertainty methodology and contact details for the current data product collection:

CH_4 bottom-up anthropogenic emissions				
Data source	**AD/Tier**	**EFs/Tier**	**Uncertainty assessment method**	**Emission data availability**
UNFCCC NGHGI (2023) CRFs and BURs	Country-specific information consistent with the IPCC GLs.	IPCC GLs/country-specific information for higher tiers.	IPCC GLs (https://www.ipcc-nggip.iges.or.jp/public/2006gl/, last access: December 2019) for calculating the uncertainty of emissions based on the uncertainty of AD and EF, two different approaches: (1) error propagation and (2) Monte Carlo simulation. The EU GHG inventory team provided yearly harmonized and gap-filled uncertainties	NGHGI official data (CRFs) are found at https://unfccc.int/ghg-inventories-annex-i-parties/2023 BUR official data are found at: https://unfccc.int/BURs For info on uncertainties please contact: Bradley Matthews bradley.matthews@umweltbundesamt.at
EDGAR v7.0	International Energy Agency (IEA) for fuel combustion Food and Agricultural Organisation (FAO) for agriculture US Geological Survey (USGS) for industrial processes (e.g. cement, lime, ammonia and ferroalloys) GGFR/NOAA for gas flaring World Steel Association for iron and steel production International Fertilisers	IPCC 2006, Tier 1 or Tier 2 depending on the sector	Tier 1 with error propagation by sectors for CH_4	https://edgar.jrc.ec.europa.eu/dataset_ghg70 CRIPPA Monica: Monica.CRIPPA@ext.ec.europa.eu

	Association (IFA) for urea consumption and production Complete description of the data sources can be found in Janssens-Maenhout et al. 2019 and in Crippa et al. (2019).			
GAINS v2020	Livestock numbers by animal type (FAOSTAT, 2010; EUROSTAT, 2009; UNFCCC, 2010) Growth in livestock numbers from FAOSTAT (2003), CAPRI model (2009) Rice cultivation Land area for rice cultivation (FAOSTAT, 2010) Projections for EU are taken from the CAPRI Model	Country-specific information and: Livestock - Implied EFs reported to UNFCCC and IPCC Tier 1 (2006, Vol.4, Ch. 10) default factors Rice cultivation - IPCC Tier 1–2 (2006, Vol. 4, p. 5.49 Agricultural waste burning - IPCC Tier 1 (2006, Vol. 5, p. 520	IPCC (2006, Vol.4, p.10.33) uncertainty range	Detailed gridded CH_4 data can be obtained by contacting the data provider: Lena Höglund Isaksson hoglund@iiasa.ac.at
FAOSTAT and PRIMAP-hist v2.4 dataset	FAOSTAT Crop and Livestock Production domains from country reporting; FAOSTAT Land Use Domain; Harmonized world soil; ESA CCI and Copernicus Global Land Cover Service (C3S) maps; MODIS MCD12Q1 v6; FAO Gridded Livestock of the World; MODIS MCD64A1.006burned area products	IPCC guidelines Tier 1	IPCC (2006, Vol.4, p.10.33) Uncertainties in estimates of GHG emissions are due to uncertainties in emission factors and activity data. They may be related to, inter alia, natural variability, partitioning fractions, lack of spatial or temporal coverage, or spatial aggregation.	Agriculture total and subdomain specific GHG emissions are found for download at https://www.fao.org/faostat/en/#data/GT (last access: November 2023). For PRIMAP-hist data contact Johannes Gütschow: mail@johannes-guetschow.de
CH_4 bottom-up natural emissions				
Data source	**AD/Tier**	**EFs/Tier**	**Uncertainty assessment method**	**Emission data availability**
CH_4 emissions from inland waters for EU27 (RECCAP2)	Hydrosheds 15s (Lehner et al., 2008) and Hydro1K (USGS, 2000) for river network, HYDROLAKES for lakes and reservoirs network and surface area (Messager et al., 2016); Worldwide	N/A	Four model configurations for CH_4	Detailed gridded data can be obtained by contacting the data providers: Ronny Lauerwald ronny.lauerwald@inrae.fr

	Typology of estuaries by Dürr et al. (2011)			
JSBACH-HIMMELI	JSBACH vegetation and soil carbon and physical parameters provided to HIMMELI to simulate wetland methane fluxes HydroLAKES database (Messager et al., 2016). CORINE land cover data VERIFY climate drivers 0.1◦ × 0.1 ◦	CH_4 fluxes from peatlands and mineral soils	the standard deviation and the resulting range in the annual emission sum represents a measure of uncertainty.	Detailed gridded data CH_4 emissions can be obtained by contacting the data providers: Tuula.Aalto@fmi.fi tiina.markkanen@fmi.fi
CH_4 emissions from global lake systems **ORNL-DAAC**	HydroLAKES and Climate Change Initiative Inland-Water (CCI-IW) remote-sensing data	N/A	N/A	Johnson, M.S. 2021. Global-Gridded Daily Methane Emissions from Inland Dam-Reservoir Systems. ORNL DAAC, Oak Ridge, Tennessee, USA. https://doi.org/10.3334/ORNLDAAC/1918
CH_4 emissions from global dam-reservoirs systems **ORNL-DAAC**	The annual duration of the emission season is based on freeze-thaw cycles of these water bodies as applicable.	N/A	N/A	https://daac.ornl.gov/cgi-bin/dsviewer.pl?ds_id=1918
Geological emissions, including marine and land geological)	Areal distribution activity: 1◦ × 1 ◦ maps include the four main categories of natural geo-CH_4 emission: (a) onshore hydrocarbon macro-seeps, including mud volcanoes, (b) submarine (offshore) seeps, (c) diffuse microseepage and (d) geothermal manifestations.	CH_4 fluxes, measurements and estimates based on size and activity	95% confidence interval of the median emission-weighted mean sum of individual regional values	Etiope et al, 2019 with updated activity for current study) Detailed gridded data on geological CH_4 emissions can be obtained by contacting the data providers: Giuseppe Etiope: giuseppe.etiope@ingv.it Giancarlo Ciotoli giancarlo.ciotoli@gmail.com

LPJ-GUESS	hydrology scheme of Wania et al. (2009) and Granberg et al. (1999). monthly wetland inundation data from the WAD2M dataset (Zhang et al., 2021). LPJ GUESS is forced with a transient climate from the CRU_ts_4.05 data set	N/A	N/A	For gridded CH_4 emissions please contact: Wenxin Zhang wenxin.zhang@nateko.lu.se
Biomass burning CH4 emissions GFEDv4.1s	The GFED4.1s data include small fires and are provided in HDF5 format. The mapped burned area is without small fires and this is the GFED4 burned area described in Giglio et al. (2013).	N/A	N/A	https://www.globalfiredata.org/ https://daac.ornl.gov/VEGETATION/guides/fire_emissions_v4_R1.html For further contacts and data please contact: Guido van der Werf guido.vanderwerf@wur.nl
CH_4 Top-down inversions				
Regional inversions over Europe (high transport model resolution)				
Data source	**AD/Tier**	**EFs/Tier**	**Uncertainty assessment method**	**Emission data availability**
FLExKF_v2023	Extended Kalman Filter in combination with backward Lagrangian transport simulations using the model FLEXPART Atmospheric observations ECMWF Era Interim meteorological fields	FLExKF-CAMSv19r_EMPA specific background	The random uncertainties are represented by the posterior error covariance matrix provided by the Kalman Filter, which combines errors in the prior fluxes with errors in the observations and model representation (see description in Appendix A1)	Detailed gridded data can be obtained by contacting the data provider: Dominik.Brunner@empa.ch
CIF CHIMERE **CIF FLEXPARTv10.4**	Extended Kalman Filter in combination with backward Lagrangian transport simulations using the model FLEXPART Atmospheric observations ECMWF Era Interim meteorological fields CHIMERE is a non-hydrostatic Eulerian chemistry-transport model		The uncertainty in each grid cell (0.25°x0.25° for CH_4) includes one due to the spatial disaggregation plus one due to emission-weighted uncertainty of a specific process.	Detailed gridded data can be obtained by contacting the data providers: Antoine Berchet antoine.berchet@lsce.ipsl.fr Espen Solum eso@nilu.no Gregoire Broquet gregoire.broquet@lsce.ipsl.fr Isabelle Pison isabelle.pison@lsce.ipsl.fr
Global inversions				

TM5-4DVAR (TROPOMI)	Global Eulerian model, using TROPOMI satellite retrievals, ERA 5 meteo and CAMS reanalysis	4DVAR variational techniques	N/A	Detailed gridded data can be obtained by contacting the data provider: Jacob van Peet j.c.a.van.peet@vu.nl Sander Houweling s.houweling@vu.nl
CTE-GCP2021	Ensemble Kalman filter Eulerian transport model TM5 ECMWF ERA-Interim meteorological data	prior fluxes from LPX-Bern DYPTOP, EDGAR v4.2 FT2010 GFED v4 Termites and ocean fluxes ground-based surface CH_4 observations GOSAT XCH_4 retrievals from NIES v2.72	The prior uncertainty is assumed to be a Gaussian probability distribution function The posterior uncertainty is calculated as standard deviation of the ensemble members, where the posterior error covariance matrix are driven by the ensemble Kalman filter.	Detailed gridded data can be obtained by contacting the data provider: aki.tsuruta@fmi.fi
CAMSv21r1 (NOAA and NOAA_GOSAT)	Bayesian inversion method observations of atmospheric mixing ratios ECMWF ERA5 re-analysis EDGAR v6.0 LPJ-wsl GFAS	Fires emission factors from Akagi et al., 2011	N/A	Detailed gridded CH_4 data can be obtained by contacting the data provider: Arjo Segers arjo.segers@tno.nl
MIROC4-ACTM (control and OH var)	Matrix inversion for calculation of fluxes from 53 and 84 partitions of the globe for CH_4 Forward model transport is nudged to JRA-55 horizontal winds and temperature.	Fire emissions for CH_4 are taken from GFEDv4s	A posteriori uncertainties are obtained from the Bayesian statistics model. A priori emissions uncertainties are uncorrelated.	Detailed gridded data can be obtained by contacting the data provider: Prabir Patra prabir@jamstec.go.jp Dmitry Belikov d.belikov@chiba-u.jp
CEOS GEOS-Chem (GOSAT) **GEOS-Chem CTM (TROPOMI) for USA only)**	Bayesian algorithm MERRA-2 meteorological fields (Gelaro et al., 2017)		Uncertainties are provided for representation (or smoothing) error and data precision but not for systematic errors in the transport model or data	Worden et al., 2022 https://acp.copernicus.org/articles/22/6811/2022/#section6 Nesser et al., 2023 https://egusphere.copernicus.org/preprints/2023/egusphere-2023-946/

CH_4 anthropogenic and natural emissions from bottom-up estimates (updates)

Data from three global datasets and models of CH_4 anthropogenic emissions inventories were used, namely: FAOSTAT, GAINS and EDGAR v7.0 (Table A1). These estimates are not completely independent from NGHGIs (see Figure 4 in Petrescu et al., 2020) as they integrate their own sectorial modelling with the UNFCCC data (e.g., common activity data and IPCC emission factors) when no other source of information is available. The CH_4 biomass and biofuel burning emissions are included in NGHGI under the UNFCCC LULUCF sector, although they are identified as a separate category by the Global Carbon Project CH_4 budget synthesis (Saunois et al., 2020).

Since 2022, FAOSTAT includes estimates for all IPCC economic sectors: Energy, IPPU, Waste and Other. These data are sourced from the PRIMAP-hist v2.4 dataset (Gütschow et al., 2022). Emissions totals from agrifood domain are computed following the Tier 1 methods of the Intergovernmental Panel on Climate Change (IPCC) Guidelines for National greenhouse gas (GHG) Inventories. Emissions from other economic sectors as defined by the IPCC are also disseminated in the domain for completeness. Emissions are calculated based on data from the UN Statistical Division (UNSD), the International Energy Agency (IEA) and other third-party. Overall, the bottom-up inventories for EU27 do a good job in capturing magnitudes and trends, particularly for Agriculture. IPPU remains the sector which is underestimated by all three EDGAR versions and we hypothesize this has to do with the mapping of activities in EDGAR compared to the UNFCCC reporting guidelines.

Compared to Petrescu et al., 2023a, in this study, we used additional natural lakes and reservoirs CH_4 emissions from the DAAC ORNL database; lakes (Johnson et al., 2022) and dam-reservoir systems (Johnson et al., 2021). More info: https://daac.ornl.gov/cgi-bin/dsviewer.pl?ds_id=1918 and https://daac.ornl.gov/CLIMATE/guides/Global_Lakes_Methane.html.

For peatlands and mineral soils in EU27, the VERIFY JSBACH-HIMMELI framework was used. For the seven global case-studies, estimates from the LPJ-GUESS model were used.

Geological emissions were initially based on the global gridded emissions from Etiope et al. 2019 and previously used in Petrescu et al., 2023a. They are updated for this study (see below).

LPJ-GUESS

In peatland soil, LPJ-GUESS uses the hydrology scheme of Wania et al. (2009) and Granberg et al. (1999), in which the water table depth is updated daily in response to precipitation, snowmelt, evapotranspiration and surface runoff. The 2m peatland soil column is subdivided into an upper 0.3 m acrotelm (within which the water table is allowed to fluctuate) above a 1.7 m permanently saturated catotelm layer. The water table is also allowed to extend above the soil surface to a maximum depth of 0.1 m. CH_4 production is simulated based on the degree of anoxia, vertical root distribution in two plant function types (i.e., floodtolerant C3 graminoids and

sphagnum mosses), and the fraction of heterotrophic respiration (Wania et al., 2010). CH4 is assumed to not be produced in dry and frozen soils. In non-peatland soils, CH_4 production is calculated as a fraction of heterotrophic respiration (Spahni et al., 2011). Methane transport includes three pathways: diffusion, plant-mediated and ebullition.

The model outputs need to be multiplied with the wetland fraction in each grid cell. The wetland fraction used used the remotely sensed monthly wetland inundation data from the WAD2M dataset (Zhang et al., 2021). This dataset comprises microwave satellite observations and static wetland maps that represent all inundated and waterlogged inland wetlands during 2000–2020. For the period 1990-2000, the wetland fraction used the value from the year 2000, which means the wetland fraction in this period is static. LPJ GUESS is forced with a transient climate (surface air temperature, total precipitation, surface incoming shortwave radiation, wetdays) from the CRU_ts_4.05 data set before a spin-up simulation of 500 years using a de-trended climate from 1901-1930.

Global geological methane emissions (with updated EU-49) and country-level breakdown, based on a global gridded seepage model

The global gridded geo-methane emission from the model of Etiope et al. (2019) has been re-calculated using the updated gridded emission from Europe (EU-49) as reported in Petrescu et al. (2023). Country-level breakdown of the global gridded emission (onshore only) has also been performed, as requested.

Table 1 summarizes the global and European geo-emission estimates derived in previous works (Etiope et al. 2019; Petrescu et al. 2023), and the updated global estimate using the EU-49 in Petrescu et al. (2023).

Table S2. Global and European geo-CH_4 emission estimates (Tg yr^{-1})

	Etiope et al (2019)	Petrescu et al (2023)	Present work
Global	37.5		
EU27			2.12
EU49 (onshore + offshore)		7.2	
EU-49 derivable from the original global grid model	13.7		
Updated global with new EU-49			31

It is important to remember that the global model of Etiope et al. (2019), exclusively targeted for gridding purposes, was based on "activity" and "emission factors" statistically derived by limited datasets, and it was mainly developed to provide the spatial distribution the geological methane sources, their CH_4 isotopic composition ($\delta^{13}C$) and potential emission intensity. Especially at continental scale, the emission values derived should, therefore, be considered only in terms of "order of magnitude". The overall uncertainties of the spatial distribution of the geo-CH_4 sources and CH_4 emissions depend on individual uncertainties of the four categories of seepage, which are discussed in Etiope et al. (2019).

Concerning the gridded country-level breakdown, we caution that splitting the global gridded emission (at 1° resolution) into individual countries is not recommended in principle, because the model uses approximative input parameters that are only acceptable at the global scale, resulting in country scale values that may not be

representative of the actual emission. In addition, the country values differ depending on whether grid cells or centroids are selected within the ArcGIS masks.

Using cells results in multiple counting of cells falling on country boundaries (so the total sum of country emissions is greater than the global), whereas using centroids results in underestimation in some countries (and in a total sum that is lower than the global). For example, for Italy, using centroids 39 cells are lost resulting in a missing emission of 106,494 ton/y. An alternative, but more laborious, solution to this problem is to "break" the cells at the boundaries, so that only the emission related to the fraction of the cell that is inside a country boundary is considered. We are evaluating this procedure in ArcGIS. However, as stated previously, this exercise does not resolve the issue of the applicability to the country level of a model that was built with parameters that have acceptable approximations only at the global scale. For this study, we used the averaged results from cells and centroids.

The annexed excel table reports five different country-levels breakdowns (geo-CH_4 emission in Tg yr^{-1}), from:

1. the global grid model (Etiope et al, 2019) reported by Worden et al (2022).
2. the global grid model (Etiope et al, 2019) using cells
3. the global grid model (Etiope et al, 2019) using centroids
4. the global grid model (Etiope et al, 2019) with updated EU-49 (Petrescu et al. 2023) using cells
5. the global grid model (Etiope et al, 2019) with updated EU-49 (Petrescu et al. 2023) using centroids

Table S3 shows the top 10 countries with higher geological methane emissions, including DR Congo and Brazil. Table S4 shows the breakdown for EU-27+UK.

As explained above, the cell-based and centroid-based breakdowns have different values. For the original global grid (without updated EU-49), the total sum of the countries does not match the global onshore emission (33.6 Tg CH_4 yr^{-1}; Etiope et al. 2019). This indicates that country-specific values must be evaluated with caution. Anyway, in all breakdowns performed, the top 10 countries are the same, with slight changes in the relative ranking of Indonesia (above China using the cells, below China using centroids).

Concerning the breakdown reported by Worden et al. (2022), we observe that all countries have an emission value (indicated as “priors” or “inventory”), with a minimum of 0.04 Tg yr^{-1}. We ignore the reason for this. Although it is not explained in Worden et al (2022), based on the total sum we assume that cell-based breakdown was applied. We also observe significant differences with the cell-based breakdown performed by us (e.g. Russia).

A further example of the limits and inadequacy of country-level breakdown from global models, is given by oddities in the top-down emission estimated in Worden et al. (2022), based on satellite data and global chemistry transport model: in some countries the derived geologic emissions (posteriors) are negative (Azerbaijan, Italy….), or 4-5 times higher than the data extracted from the global model of Etiope et al. (2019) without reasonable motivation (e.g., Japan). Worden et al (2022) admit that “*given the co-location of seep emissions with oil and coal, care must be taken in interpreting our results for seep emissions estimates”.*

Table S3. Top 10 countries resulting with the highest geo-CH_4 emission (emission in Tg yr^{-1}) in the several breakdowns (performed by Worden et al , 2022; performed by us using the original Etiope et al (2019) global grid using cells and centroids; performed using the global model with updated EU-49 grid (Petrescu et al. 2023). Brazil and DR Congo are also reported as requested.

Breakdown by Worden et al (2022)		**Breakdown using cells**			**Breakdown using centroids**			**Breakdown with updated EU49 using cells**			**Breakdown with updated EU49 using centroids**		
Country	Emission	Country	Emission	N.Cells	Country	Emission	N.Centroids	Country	Emission	N.Cells	Country	Emission	N.Centroids
USA	6.7	USA	7.46	1377	USA	6.53	1108	USA	7.46	1377	USA	6.53	1108
Russian Fed.	2.6	Russian Federation	3.72	3485	Russian Fed.	2.19	2939	Russian Fed.	2.86	3485	Russian Fed.	1.67	2939
Azerbaijan	2.8	Azerbaijan	2.95	31	Azerbaijan	2.74	18	Azerbaijan	2.36	31	Azerbaijan	2.26	18
Canada	1.1	Canada	1.38	2261	Canada	1.11	1709	Canada	1.38	2261	Canada	1.11	1709
Indonesia	0.62	Indonesia	1.28	371	Indonesia	0.96	152	Indonesia	1.28	371	Indonesia	0.96	152
China	1	China	1.26	1095	China	1.21	952	China	1.26	1095	China	1.21	952
Italy	2.9	Italy	2.99	74	Italy	2.69	35	Italy	1.11	74	Italy	1.01	35
Romania	2.1	Romania	2.27	46	Romania	2	26	Romania	0.94	46	Romania	0.83	26
Japan	0.96	Japan	0.91	95	Japan	0.59	34	Japan	0.91	95	Japan	0.59	34
Venezuela	0.66	Venezuela	0.76	108	Venezuela	0.55	75	Venezuela	0.76	108	Venezuela	0.55	75
Brazil	0.06	Brazil	0.08	813	Brazil	0.06	705	Brazil	0.08	813	Brazil	0.06	705
DR Congo	0.04	DR Congo	0.07	236	DR Congo	0.02	188	DR Congo	0.07	236	DR Congo	0.02	188

Table S4. Country-level breakdown for EU-27+UK, after updates in Petrescu et al. (2023). Emission in Tg yr^{-1}.

Country	**Centroids**	**Emission**
Austria	12	0.05
Belgium	3	0.00
Bulgaria	12	0.01
Croatia	7	0.01
Cyprus	0	0.00
Czech Repub	9	0.03
Denmark	8	0.00
Estonia	6	0.00
Finland	65	0.00
France	66	0.03
Germany	44	0.03
Greece	12	0.02
Hungary	10	0.02
Ireland	8	0.00
Italy	**36**	**1.01**
Latvia	12	0.00
Lithuania	9	0.00
Luxembourg	0	0.00
Malta	0	0.00
Netherlands	5	0.00
Poland	41	0.05
Portugal	13	0.00
Romania	**25**	**0.83**
Slovakia	5	0.02
Slovenia	2	0.00
Spain	50	0.01
Sweden	77	0.00
UK	33	0.06

CH_4 emission data from inversions

Atmospheric inversions optimize prior estimates of emissions and sinks through modeling frameworks that utilizes atmospheric observations as a constraint on fluxes. Emission estimates from inversions depend on the data set of atmospheric measurements and the choice of the atmospheric model, as well as on other inputs (e.g., prior emissions and their uncertainties). Some of the inversions allow for explicit attribution to different sectors, while others optimize all fluxes in each grid cell and then attribute emissions to sectors using prior grid-cell fractions

(see details in Saunois et al. 2020 for global inversions). For CH_4, regional inversions were used for EU27 estimates while global inversion frameworks were used for the seven global case-studies (Table 2).

Descriptions of approaches are found in Petrescu et al., 2023a, Appendix A1.2. The new approaches are described below:

CAMSv21r1

The CAMS global methane flux inversion system provides time series of gridded CH_4 emission estimates that are updated every year. The release v21r1 used in this study was produced in 2022 and covers the time period 1979-2021 (Segers et al., 2022). Emissions are estimated using the TM5-4DVAR inversion system that uses surface and eventually also satellite observations to constrain the emissions.

The inversion system is built around the TM5 global tracer transport model (Huijnen et al., 2010). In this application the model uses meteorological data from the ECMWF ERA5 re-analysis to simulate gridded mixing ratios of CH_4. A horizontal model resolution of 3^ox2^o degrees is used, with 34 vertical layers that are defined as a coarsening of the orginal ERA5 layers. Physical processes include emission, advection, convection and vertical diffusion, and chemical reactions. The chemical desctruction of CH4 is described using offline computed mixing ratios of OH and in the stratosphere also of $O(^1D)$ and Cl^- obtained from various simulations with the CAMS global chemistry model.

The inversion system optimized four groups of emissions. The largest emissions are the anthropogenic emissions that are taken from EDGAR v6.0 (Crippa et al., 2021), which provides global gridded emissions at monthly temporal resolution. This emission group also contains some smaller sources from oceans, wild animals, and termites, and the soil sink. Emissions from rice paddies are considered a sepeate group and also these are taken from EDGAR v6.0. The third emission group is formed by wetland emissions which are taken from simulations with the LPJ-wsl model (Zhang et al., 2018). Emissions from biomass burning are taken from GFAS (Kaiser et al., 2012) as fourth group. Emissions are optimized at monthly resolution. An *a priori* unceratainty of 50% is assumed for the antropogenic sources and 100% for the other. A horizontal correlation is assumed with a length scale of 500 km, and for the anthropogenic sources also a temporal correlation is assumed with a length scale of 9.5 months.

In a first inversion, only urface observations are used to constrain the emissions. The observations are taken from remote locations in the NOAA network (Lan et al., 2022), where the observation representation errors are parameterized following (Bergamaschi et al., 2010). In a second inversion, also column mixing ratio's from the GOSAT satellite instrument are taken into account over the period 2009-2021 (Parker and Boesch, 2020). When comparing the GOSAT columns with the TM5 simulations, a bias correction is applied that was derived from the surface-only *posterior* simulations, to ensure that simulations at the surface are kept in agreement with the NOAA observations. Each of the emission time series are optimized in a single inversion, employing a temporal parallelization scheme (Pandey et al, 2022). The results are evaluated by comparison with surface observations that are not used in the inversion, FTIR profiles, satellite retrievals, and air craft observations.

TM5-4DVAR and TROPOMI data

Within the ESA Methane+ project[1], CH_4 inversions were performed using TM5-4DVAR and TROPOMI data. TM5-4DVAR is a version of the TM5-model[2] (e.g. Huijnen et al., 2010) developed for 4DVAR data assimilation of satellite and surface observations of CH_4. In the setup used here, the model runs from 1-1-2018 till 1-4-2021, but the output is validated from 1-5-2018 till 1-1-2021 to allow for spin-up and spin-down. The model runs on a horizontal grid of 6 × 4 degree (longitude × latitude) and ERA 5 meteo is used to drive the model. The 4 source categories that are being optimised ("biomass burning", "rice", "wetlands", and "other") are the same as in the CAMS reanalysis and have distinct spatio-temporal properties so that the inversion algorithm can distinguish their effect on the CH_4 concentration. The initial concentration field is derived from a CAMS inversion using surface measurements only (version v20r1) and is not updated in the inversion.

The SRON scientific TROPOMI product has been used in the inversion (Lorente et al., 2023), which uses a 3rd order polynomial fit to correct some artefacts that were caused by spectral features of the underlying surfaces. Only cloud-free retrievals have been used, and a bias correction has been applied based on an inversion using only surface data. The retrievals were then combined into super observations with the same resolution as the model grid, using a weighted average based on the uncertainty provided in the data product.

CTE-GCP2021 USA trends

The CTE-GCP2021 inverse model was run with both EDGAR and GAINS prior information. We will investigate here Western and Eastern regions in the USA (Figure S1)

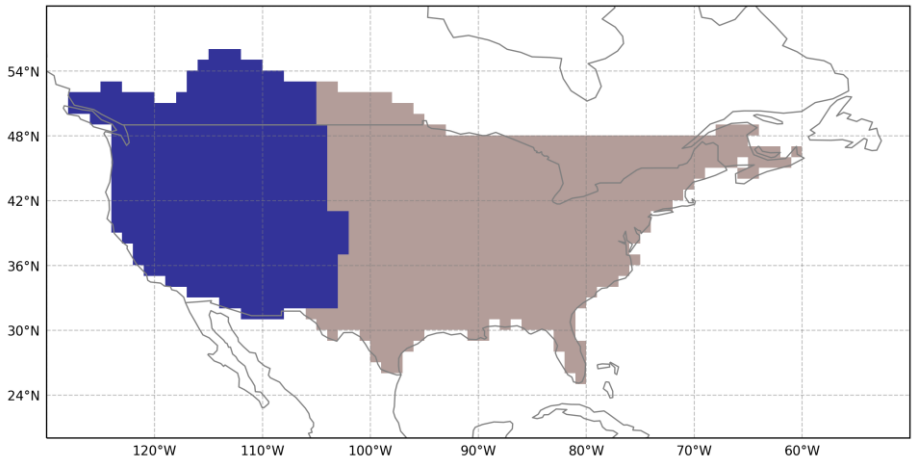

Figure S1: Western (blue) and eastern (brown) regions of USA where regional emission estimates are investigated.

In Western USA, oil & gas emissions are increased from the GAISN prior (dotted red), and the increasing trend in GAINS CH_4 emissions are as well pronounced in the posterior estimates (full red) with magnitudes between 8 – 18 Tg CH_4 yr^{-1} from 2000-2020 (Figure S2). Both prior and posterior from EDGAR (black) keep a flat trend. In both cases, the posteriors follow the prior trends.

1 https://methaneplus.eu/
2 https://tm5.site.pro/

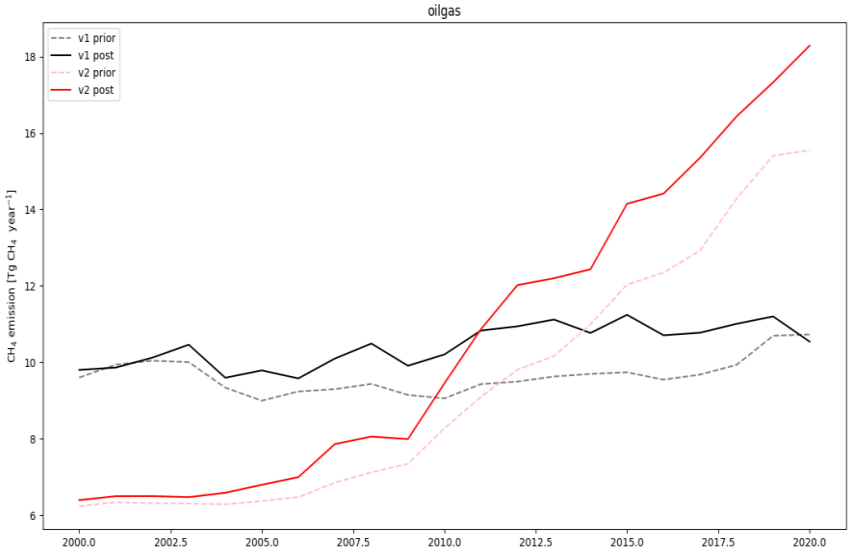

Figure S2: Western USA comparison between oil and gas emissions from CTE-GCP2021 runs using EDGAR (v1 black) and GAINS(v2 red) priors.

In Eastern USA, where the Permian basin is located, the oil & gas emission magnitude is very different for the GAINS priors (40 – 120 Tg CH_4 yr^{-1}) (Figure S3), showing a similar increasing trend between 2000-2020 as the Eastern part. The run using EDGAR as prior registers a high jump in 2010. Also in this region, the posteriors are following the priors.

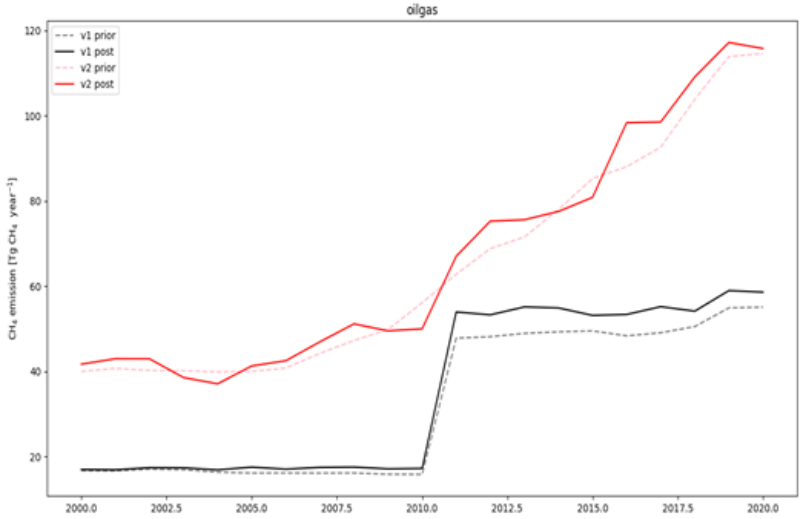

Figure S3: Eastern USA comparison between oil and gas emissions from CTE-GCP2021 runs using EDGAR (v1 black) and GAINS(v2 red) priors.

In both regions, posterior emissions are higher for coal and show decreasing trends, and this triggers a stronger increasing trend in total emissions for the runs using GAINS (Figures S4).

Figure S4: Eastern (left) and Western (right) USA comparison between CTE-GCP2021 total CH_4 emissions using EDGAR (v1 black) and GAINS(v2 red) priors.

It is still under investigation if the atmospheric observations have a role and might induce as well such an abrupt increased trend in the runs using GAINS as prior.

References:

Berchet, A., Sollum, E., Thompson, R. L., Pison, I., Thanwerdas, J., Broquet, G., Chevallier, F., Aalto, T., Berchet, A., Bergamaschi, P., Brunner, D., Engelen, R., Fortems-Cheiney, A., Gerbig, C., Groot Zwaaftink, C. D., Haussaire, J.-M., Henne, S., Houweling, S., Karstens, U., Kutsch, W. L., Luijkx, I. T., Monteil, G., Palmer, P. I., van Peet, J. C. A., Peters, W., Peylin, P., Potier, E., Rödenbeck, C., Saunois, M., Scholze, M., Tsuruta, A., and Zhao, Y.: The Community Inversion Framework v1.0: a unified system for atmospheric inversion studies, Geosci. Model Dev., 14, 5331–5354, https://doi.org/10.5194/gmd-14-5331-2021, 2021.

Bergamaschi, P., Krol, M., Meirink, J. F., Dentener, F., Segers, A., van Aardenne, J., Monni, S., Vermeulen, A. T., Schmidt, M., Ramonet, M., Yver, C., Meinhardt, F., Nisbet, E. G., Fisher, R. E., O'Doherty, S., & Dlugokencky, E. J.: Inverse modeling of European CH_4 emissions 2001-2006. *Journal of Geophysical Research*, *115*(D22), D22309. https://doi.org/10.1029/2010JD014180, 2010.

Bruhwiler, L., Dlugokencky, E., Masarie, K., Ishizawa, M., Andrews, A., Miller, J., Sweeney, C., Tans, P. and Worthy, D.: CarbonTracker-CH4: an assimilation system for estimating emissions of atmospheric methane, Atmos. Chem. Phys., 14(16), 8269–8293, doi:10.5194/acp-14-8269-2014, 2014.

Brunner, D., Arnold, T., Henne, S., Manning, A., Thompson, R. L., Maione, M., O'Doherty, S., and Reimann, S.: Comparison of four inverse modelling systems applied to the estimation of HFC-125, HFC-134a, and SF6 emissions over Europe, Atmos. Chem. Phys., 17, 10651–10674, https://doi.org/10.5194/acp-17-10651-2017, 2017.

Brunner, D., Henne, S., Keller, C. A., Reimann, S., Vollmer, M. K., O'Doherty, S., and Maione, M.: An extended Kalman-filter for regional scale inverse emission estimation, Atmos. Chem. Phys., 12, 3455–3478, https://doi.org/10.5194/acp-12-3455-2012, 2012.

Chandra, Naveen., Patra, P., Bisht, J., Ito, A., Umezawa, T., Saigusa, N., Morimoto, S., Aoki, S., Janssens-Maenhout, G., Fujita, R., Takigawa, M., Watanabe, S., Saitoh, N. and Canadell, J.G., Emissions from the oil and gas sectors, coal mining and ruminant farming drive methane growth over the past three decades, JOURNAL OF THE METEOROLOGICAL SOCIETY OF JAPAN, ISSN 0026-1165, 99 (2), p. 309-337, JRC123075, 2021.

Crippa, M., Oreggioni, G., Guizzardi, D., Muntean, M., Schaaf, E., Lo Vullo, E., Solazzo, E., Monforti-Ferrario, F., Olivier, J. G. J., and Vignati, E.: Fossil CO_2 and GHG emissions of all world countries – 2019 Report, EUR 29849 EN, Publications Office of the European Union, Luxembourg, ISBN 978-92-76-11100-9, https://doi.org/10.2760/687800, JRC117610, 2019.

Crippa, M., Solazzo, E., Huang, G., Guizzardi, D., Koffi, E. N., Muntean, M., Schieberle, C., Friedrich, R., and Janssens-Maenhout, G.: Towards time varying emissions: development of high resolution temporal profiles in the Emissions Database for Global Atmospheric Research, Sci. Data., 7, 121, https://doi.org/10.1038/s41597-020-0462-2, 2020.

Crippa, Monica, Guizzardi, D., Muntean, M., Schaaf, E., Lo Vullo, E., Solazzo, E., Monforti-Ferrario, F., Olivier, J., & Vignati, E.: *EDGAR v6.0 Greenhouse Gas Emissions*. http://data.europa.eu/89h/97a67d67-c62e-4826-b873-9d972c4f670b, 2021.

D8.2 $CoCO_2$ project: Second synthesis of CO_2 and CH_4 observation-based emission estimates, https://coco2-project.eu/node/360, 2022.

Etiope, G., Ciotoli, G., Schwietzke, S., and Schoell, M.: Gridded maps of geological methane emissions and their isotopic signature, Earth Syst. Sci. Data, 11, 1–22, https://doi.org/10.5194/essd-11-1-2019, 2019.

FAO: FAOSTAT, Statistics Division of the Food and Agricultural Organisation of the UN, statistics till 2021: https://www.fao.org/faostat/en/#data/GT (last access November 2023), 2023.

FAO: The State of Food and Agriculture: Social protection and agriculture: breaking the cycle of rural poverty, 2015, Rome, Italy, http://www.fao.org/3/a-i4910e.pdf (last access: September 2023), 2015.

Fortems-Cheiney, A., Pison, I., Broquet, G., Dufour, G., Berchet, A., Potier, E., Coman, A., Siour, G., and Costantino, L.: Variational regional inverse modeling of reactive species emissions with PYVAR-CHIMERE-v2019, Geosci. Model Dev., 14, 2939–2957, https://doi.org/10.5194/gmd-14-2939-2021, 2021.

Gelaro, R., McCarty, W., Suárez, M. J., Todling, R., Molod, A., Takacs, L., Randles, C. A., Darmenov, A., Bosilovich, M. G., Reichle, R., Wargan, K., Coy, L., Cullather, R., Draper, C., Akella, S., Buchard, V., Conaty,

A., da Silva, A. M., Gu, W., Kim, G.-K., Koster, R., Lucchesi, R., Merkova, D., Nielsen, J. E., Partyka, G., Pawson, S., Putman, W., Rienecker, M., Schubert, S. D., Sienkiewicz, M., and Zhao, B.: The Modern-Era Retrospective Analysis for Research and Applications, Version 2 (MERRA-2), J. Climate, 30, 5419–5454, https://doi.org/10.1175/jcli-d-16-0758.1, 2017.

Giglio, L., Randerson, J. T., and van der Werf, G. R.: Analysis of daily, monthly, and annual burned area using the fourth-generation global fire emissions database (GFED4), J. Geophys. Res.-Biogeo., 118, 317–328, https://doi.org/10.1002/jgrg.20042, 2013.

Gütschow, J. and Pflüger, M.: The PRIMAP-hist national historical emissions time series (1750-2021) v2.4. Zenodo: https://doi.org/10.5281/zenodo7179775, 2022.

Höglund-Isaksson L., Gómez-Sanabria, A., Klimont, Z., Rafaj, P., and Schöpp, W.: Technical potentials and costs for reducing global anthropogenic methane emissions in the 2050 timeframe – results from the GAINS model, Environ. Res. Commun., 2, 025004, https://doi.org/10.1088/2515-7620/ab7457, 2020.

Höglund-Isaksson, L.: Bottom-up simulations of methane and ethane from global oil and gas systems, Environ. Res. Lett., 12, 024007, https://doi.org/10.1088/1748-9326/aa583e, 2017.

Houweling, S., Krol, M., Bergamaschi, P., Frankenberg, C., Dlugokencky, E. J., Morino, I., Notholt, J., Sherlock, V., Wunch, D., Beck, V., Gerbig, C., Chen, H., Kort, E. A., Röckmann, T., and Aben, I.: A multi-year methane inversion using SCIAMACHY, accounting for systematic errors using TCCON measurements, Atmos. Chem. Phys., 14, 3991–4012, https://doi.org/10.5194/acp-14-3991-2014, 2014.

Huijnen, V., Williams, J., van Weele, M., van Noije, T., Krol, M., Dentener, F., Segers, A., Houweling, S., Peters, W., de Laat, J., Boersma, F., Bergamaschi, P., van Velthoven, P., Le Sager, P., Eskes, H., Alkemade, F., Scheele, R., Nédélec, P., & Pätz, H.-W.: The global chemistry transport model TM5: description and evaluation of the tropospheric chemistry version 3.0. *Geoscientific Model Development*, *3*(2), 445–473. https://doi.org/10.5194/gmd-3-445-2010, 2010.

Ito, A. and Inatomi, M.: Use of a process-based model for assessing the methane budgets of global terrestrial ecosystems and evaluation of uncertainty, Biogeosciences, 9, 759–773, https://doi.org/10.5194/bg-9-759-2012, 2012.

Janssens-Maenhout, G., Crippa, M., Guizzardi, D., Muntean, M., Schaaf, E., Dentener, F., Bergamaschi, P., Pagliari, V., Olivier, J. G. J., Peters, J. A. H. W., van Aardenne, J. A., Monni, S., Doering, U., Petrescu, A. M. R., Solazzo, E., and Oreggioni, G. D.: EDGAR v4.3.2 Global Atlas of the three major greenhouse gas emissions for the period 1970–2012, Earth Syst. Sci. Data, 11, 959–1002, https://doi.org/10.5194/essd-11-959-2019, 2019.

Janssens-Maenhout, G., Pagliari, V., Guizzardi, D., and Muntean, M.: Global emission inventories in the Emission Database for Global Atmospheric Research (EDGAR) – Manual (I) I. Gridding: EDGAR emissions distribution on global gridmaps, EUR – Scientific and Technical Research Reports, Publications Office of the European Union, http://publications.jrc.ec.europa.eu/repository/bitstream/JRC78261/edgarv4_manual_i_gridding_pubsy_final.pdf (last access: 7 February 2018), 2013.

Johnson, M.S., Matthews, E., Bastviken, D., Du, J., and Genovese, V.: Global-Gridded Daily Methane Emissions Climatology from Lake Systems, 2003-2015. ORNL DAAC, Oak Ridge, Tennessee, USA. https://doi.org/10.3334/ORNLDAAC/2008, 2022.

Johnson, M.S.: Global-Gridded Daily Methane Emissions from Inland Dam-Reservoir Systems. ORNL DAAC, Oak Ridge, Tennessee, USA. https://doi.org/10.3334/ORNLDAAC/1918, 2021.

Kaiser, J. W., Heil, A., Andreae, M. O., Benedetti, A., Chubarova, N., Jones, L., Morcrette, J.-J., Razinger, M., Schultz, M. G., Suttie, M., & van der Werf, G. R.: Biomass burning emissions estimated with a global fire assimilation system based on observed fire radiative power. *Biogeosciences*, *9*(1), 527–554. https://doi.org/10.5194/bg-9-527-2012, 2012.

Krol, M., Houweling, S., Bregman, B., van den Broek, M., Segers, A., van Velthoven, P., Peters, W., Dentener, F., and Bergamaschi, P.: The two-way nested global chemistry-transport zoom model TM5: algorithm and applications, Atmos. Chem. Phys., 5, 417–432, https://doi.org/10.5194/acp-5-417-2005, 2005.

Lauerwald, R., Allen, G. H., Deemer, B. R., Liu, S., Maavara, T., Raymond, P., et al.: Inland water greenhouse gas budgets for RECCAP2: 2. Regionalization and homogenization of estimates. *Global Biogeochemical Cycles*, **37**(5), e2022GB007658. https://doi.org/10.1029/2022gb007658, 2023.

Lorente, A., Borsdorff, T., Martinez-Velarte, M. C., and Landgraf, J.: Accounting for surface reflectance spectral features in TROPOMI methane retrievals, Atmos. Meas. Tech., 16, 1597–1608, https://doi.org/10.5194/amt-16-1597-2023, 2023.

Nesser, H., Jacob, D. J., Maasakkers, J. D., Lorente, A., Chen, Z., Lu, X., Shen, L., Qu, Z., Sulprizio, M. P., Winter, M., Ma, S., Bloom, A. A., Worden, J. R., Stavins, R. N., and Randles, C. A.: High-resolution U.S. methane emissions inferred from an inversion of 2019 TROPOMI satellite data: contributions from individual states, urban areas, and landfills, EGUsphere [preprint], https://doi.org/10.5194/egusphere-2023-946, 2023.

Pandey, S, Houweling, S., & Segers, A.: Order of magnitude wall time improvement of variational methane inversions by physical parallelization: a demonstration using TM5-4DVAR. *Geosci. Model Dev.*, *15*(11), 4555–4567. https://doi.org/10.5194/gmd-15-4555-2022, 2022.

Pandey, S., Houweling, S., Krol, M., Aben, I., Chevallier, F., Dlugokencky, E. J., Gatti, L. V., Gloor, E., Miller, J. B., Detmers, R., Machida, T., and Röckmann, T.: Inverse modeling of GOSAT-retrieved ratios of total column CH_4 and CO_2 for 2009 and 2010, Atmos. Chem. Phys., 16, 5043–5062, https://doi.org/10.5194/acp-16-5043-2016, 2016.

Parker, R.; Boesch, H.: University of Leicester GOSAT Proxy XCH4 v9.0. Centre for Environmental Data Analysis, 07 May 2020. doi:10.5285/18ef8247f52a4cb6a14013f8235cc1eb. https://dx.doi.org/10.5285/18ef8247f52a4cb6a14013f8235cc1eb, 2020.

Patra, P.K., Krol, M.C., Prinn, R.G., Takigawa, M., Muhle, J., Montzka, S., Lal, S., Yamashita, Y., Naus, S., Chandra, N., Weiss, R.F., Krummerl, P.B., Fraser, P.J., O'Doherty, S., Elkins, J.W.: Methyl Chloroform Continues to Constrain the Hydroxyl (OH) Variability in the Troposphere. Journal of Geophysical Research: Atmospheres, 126(4), e2020JD033862, doi: 10.1029/2020jd033862, 2021.

Peters, W., Miller, J. B., Whitaker, J., Denning, A. S., Hirsch, A., Krol, M. C., Zupanski, D., Bruhwiler, L., and Tans, P. P.: An ensemble data assimilation system to estimate CO_2 surface fluxes from atmospheric trace gas observations, J. Geophys. Res., 110, D24304, https://doi.org/10.1029/2005JD006157, 2005.

Petrescu, A. M. R., Qiu, C., McGrath, M. J., Peylin, P., Peters, G. P., Ciais, P., Thompson, R. L., Tsuruta, A., Brunner, D., Kuhnert, M., Matthews, B., Palmer, P. I., Tarasova, O., Regnier, P., Lauerwald, R., Bastviken, D., Höglund-Isaksson, L., Winiwarter, W., Etiope, G., Aalto, T., Balsamo, G., Bastrikov, V., Berchet, A., Brockmann, P., Ciotoli, G., Conchedda, G., Crippa, M., Dentener, F., Groot Zwaaftink, C. D., Guizzardi, D., Günther, D., Haussaire, J.-M., Houweling, S., Janssens-Maenhout, G., Kouyate, M., Leip, A., Leppänen, A., Lugato, E., Maisonnier, M., Manning, A. J., Markkanen, T., McNorton, J., Muntean, M., Oreggioni, G. D., Patra, P. K., Perugini, L., Pison, I., Raivonen, M. T., Saunois, M., Segers, A. J., Smith, P., Solazzo, E., Tian, H., Tubiello, F. N., Vesala, T., van der Werf, G. R., Wilson, C., and Zaehle, S.: The consolidated European synthesis of CH_4 and N_2O emissions for the European Union and United Kingdom: 1990–2019, Earth Syst. Sci. Data, 15, 1197–1268, https://doi.org/10.5194/essd-15-1197-2023, 2023a.

Petrescu, A.M.R., Peters, G.P., Engelen, R., Houweling, S., Brunner, D., Tsuruta, A., Matthews, B., Patra, P.K., Belikov, D., Thompson, R.L., Höglund-Isaksson, L., Zhang, W., Segers, A.J., Etiope, G., Ciotoli, G., Peylin, P., Chevallier, F., Aalto, T., Andrew, R.M., Bastviken, D., Berchet, A., Broquet, G., Conchedda, G., Gütschow, J., Haussaire, J.-M., Lauerwald, R., Markkanen, T., van Peet, J.C.A., Pison, I., Regnier, P., Solum, E., Scholze, M., Tenkanen, M., Tubiello, F.N., van der Werf, G.R., Worden, J.R.: Reconciliation of observation- and inventory-based CH4 emissions for eight large global emitters, version 1, Zenodo [data set], https://doi.org/10.5281/zenodo.10276087, 2023b.

Raivonen, M., Smolander, S., Backman, L., Susiluoto, J., Aalto, T., Markkanen, T., Mäkelä, J., Rinne, J., Peltola, O., Aurela, M., Lohila, A., Tomasic, M., Li, X., Larmola, T., Juutinen, S., Tuittila, E.-S., Heimann, M., Sevanto, S., Kleinen, T., Brovkin, V., and Vesala, T.: HIMMELI v1.0: HelsinkI Model of MEthane buiLd-up and emIssion for peatlands, Geosci. Model Dev., 10, 4665–4691, https://doi.org/10.5194/gmd-10-4665-2017, 2017.

Saunois, M., Stavert, A. R., Poulter, B., Bousquet, P., Canadell, J. G., Jackson, R. B., Raymond, P. A., Dlugokencky, E. J., Houweling, S., Patra, P. K., Ciais, P., Arora, V. K., Bastviken, D., Bergamaschi, P., Blake, D. R., Brailsford, G., Bruhwiler, L., Carlson, K. M., Carrol, M., Castaldi, S., Chandra, N., Crevoisier, C., Crill, P. M., Covey, K., Curry, C. L., Etiope, G., Frankenberg, C., Gedney, N., Hegglin, M. I., Höglund-Isaksson, L., Hugelius, G., Ishizawa, M., Ito, A., Janssens-Maenhout, G., Jensen, K. M., Joos, F., Kleinen, T., Krummel, P. B., Langenfelds, R. L., Laruelle, G. G., Liu, L., Machida, T., Maksyutov, S., McDonald, K. C., McNorton, J., Miller, P. A., Melton, J. R., Morino, I., Müller, J., Murguia-Flores, F., Naik, V., Niwa, Y., Noce, S., O'Doherty, S., Parker, R. J., Peng, C., Peng, S., Peters, G. P., Prigent, C., Prinn, R., Ramonet, M., Regnier, P., Riley, W. J., Rosentreter, J. A., Segers, A., Simpson, I. J., Shi, H., Smith, S. J., Steele, L. P., Thornton, B. F., Tian, H., Tohjima, Y., Tubiello, F. N., Tsuruta, A., Viovy, N., Voulgarakis, A., Weber, T. S., van Weele, M., van der Werf, G. R., Weiss, R. F., Worthy, D., Wunch, D., Yin, Y., Yoshida, Y., Zhang, W., Zhang, Z., Zhao, Y., Zheng, B., Zhu, Q., Zhu, Q., and Zhuang, Q.: The Global Methane Budget 2000–2017, Earth Syst. Sci. Data, 12, 1561–1623, https://doi.org/10.5194/essd-12-1561-2020, 2020.

Segers, A.J.: Description of the CH_4 Inversion Production Chain, https://atmosphere.copernicus.eu/sites/default/files/2021-01/CAMS73_2018SC3_D73.5.2.2-2020_202012_production_chain_Ver1.pdf, 2020.

Segers, A.J.: Validation of the CH_4 surface flux inversion – reanalysis 1990–2019, Document Title (copernicus.eu), https://atmosphere.copernicus.eu/sites/default/files/2021-02/CAMS73_2018SC2_D73.2.4.1-2020_202012_validation_CH4_1990-2019_v2.pdf (last access: June 2023), 2020.

Segers, A.J., Steinke, T., Houweling, S.: Evaluation and Quality Control document for observation-based CH_4 flux estimates for the period 1979-2021. CAMS report D55.2.4.1-2022, 2022.

Solazzo, E., Crippa, M., Guizzardi, D., Muntean, M., Choulga, M., and Janssens-Maenhout, G.: Uncertainties in the Emissions Database for Global Atmospheric Research (EDGAR) emission inventory of greenhouse gases, Atmos. Chem. Phys., 21, 5655–5683, https://doi.org/10.5194/acp-21-5655-2021, 2021.

Spahni, R., Wania, R., Neef, L., van Weele, M., Pison, I., Bousquet, P., Frankenberg, C., Foster, P. N., Joos, F., Prentice, I. C., and van Velthoven, P.: Constraining global methane emissions and uptake by ecosystems, Biogeosciences, 8, 1643–1665, https://doi.org/10.5194/bg-8-1643-2011, 2011.

Stocker, B. D., Spahni, R., and Joos, F.: DYPTOP: a cost-efficient TOPMODEL implementation to simulate sub-grid spatio-temporal dynamics of global wetlands and peatlands, Geosci. Model Dev., 7, 3089–3110, https://doi.org/10.5194/gmd-7-3089-2014, 2014.

Susiluoto, J., Raivonen, M., Backman, L., Laine, M., Makela, J., Peltola, O., Vesala, T., and Aalto, T.: Calibrating the sqHIMMELI v1.0 wetland methane emission model with hierarchical modeling and adaptive MCMC, Geosci. Model Dev., 11, 1199–1228, https://doi.org/10.5194/gmd-11-1199-2018, 2018.

Tubiello, F. N., Karl, K., Flammini, A., Gütschow, J., Obli-Laryea, G., Conchedda, G., Pan, X., Qi, S. Y., Halldórudóttir Heiðarsdóttir, H., Wanner, N., Quadrelli, R., Rocha Souza, L., Benoit, P., Hayek, M., Sandalow, D., Mencos Contreras, E., Rosenzweig, C., Rosero Moncayo, J., Conforti, P., and Torero, M.: Pre- and post-production processes increasingly dominate greenhouse gas emissions from agri-food systems, Earth Syst. Sci. Data, 14, 1795–1809, https://doi.org/10.5194/essd-14-1795-2022, 2022.

Tubiello, F. N., Salvatore, M., Rossi, S., Ferrara, A., Fitton, N., and Smith, P.: The FAOSTAT database of greenhouse gas emissions from agriculture, Environ. Res. Lett., 8, 015009, https://doi.org/10.1088/1748-326/8/1/015009, 2013.

Tubiello, F. N.: Greenhouse Gas Emissions Due to Agriculture, Enc. Food Security Sustain., 1, 196–205, https://doi.org/10.1016/B978-0-08-100596-5.21996-3, 2019.

van der Werf, G. R., Randerson, J. T., Giglio, L., van Leeuwen, T. T., Chen, Y., Rogers, B. M., Mu, M., van Marle, M. J. E., Morton, D. C., Collatz, G. J., Yokelson, R. J., and Kasibhatla, P. S.: Global fire emissions estimates during 1997–2016, Earth Syst. Sci. Data, 9, 697–720, https://doi.org/10.5194/essd-9-697-2017, 2017.

Wania, R., Ross, I., and Prentice, I. C.: Implementation and evaluation of a new methane model within a dynamic global vegetation model: LPJ-WHyMe v1.3.1, Geosci. Model Dev., 3, 565–584, https://doi.org/10.5194/gmd-3-565-2010, 2010.

Wania, R., Ross, I., and Prentice, I. C.: Integrating peatlands and permafrost into a dynamic global vegetation model: 1. Evaluation and sensitivity of physical land surface processes, *Global Biogeochem. Cycles*, 23, GB3014, doi:10.1029/2008GB003412, 2009.

Worden, J. R., Cusworth, D. H., Qu, Z., Yin, Y., Zhang, Y., Bloom, A. A., ... & Jacob, D. J.: The 2019 methane budget and uncertainties at 1° resolution and each country through Bayesian integration Of GOSAT total column methane data and a priori inventory estimates. Atmospheric Chemistry and Physics, 22(10), 6811-6841, https://doi.org/10.5194/acp-22-6811-2022, 2022.

Zhang, Z., Fluet-Chouinard, E., Jensen, K., McDonald, K., Hugelius, G., Gumbricht, T., Carroll, M., Prigent, C., Bartsch, A., and Poulter, B.: Development of the global dataset of Wetland Area and Dynamics for Methane Modeling (WAD2M) , Earth Syst. Sci. Data, 13, 2001–2023, https://doi.org/10.5194/essd-13-2001-2021, 2021.

Zhang, Z., Zimmermann, N. E., Calle, L., Hurtt, G., Chatterjee, A., & Poulter, B.: Enhanced response of global wetland methane emissions to the 2015-2016 El Niño-Southern Oscillation event. *Environmental Research Letters*, *13*(7). https://doi.org/10.1088/1748-9326/aac939, 2018.